Robust Pipeline Localization for an Autonomous Underwater Vehicle using Stereo Vision and Echo Sounder Data

Gøril M. Breivik, Sigurd A. Fjerdingen and Øystein Skotheim

SINTEF, P.O.Box 124 Blindern, N-0314 Oslo, Norway

ABSTRACT

Submarine oil and gas pipeline inspection is a highly time and cost consuming task. Using an autonomous underwater vehicle (AUV) for such applications represents a great saving potential. However, the AUV navigation system requires reliable localization and stable tracking of the pipeline position. We present a method for robust pipeline localization relative to the AUV in 3D based on stereo vision and echo sounder depth data. When the pipe is present in both camera images, a standard stereo vision approach is used for localization. Enhanced localization continuity is ensured using a second approach when the pipe is segmented out in only one of the images. This method is based on a combination of one camera with depth information from the echo sounder mounted on the AUV. In the algorithm, the plane spanned by the pipe in the camera image is intersected with the plane spanned by the sea floor, to give the pipe position in 3D relative to the AUV. Closed water recordings show that the proposed method localizes the pipe with an accuracy comparable to that of the stereo vision method. Furthermore, the introduction of a second pipe localization method increases the true positive pipe localization rate by a factor of four.

Keywords: stereo vision, echo sounder, autonomous underwater vehicle, AUV, robust localization, pipe inspection, robot vision, scene analysis

1. INTRODUCTION

Submarine pipelines are one of the most important network structures of the oil and gas industry, connecting for instance offshore installations to onshore processing plants. The length of pipelines in the North Sea alone supersedes 20000 km, and as an example of cost, the 1200 km long Langeled pipeline was priced at 3200 million USD.[1] Pipeline shutdowns due to deteriorating conditions are costly, and national regulations usually require some form of integrity check of pipelines to prevent environmental harm.

There is a need to inspect these submarine structures in order to obtain some assessment of integrity. Main pipeline defects include corrosion and anode depletion, cracking, stress, bending and denting, in addition to irregularities such as movements with respect to the last inspection, free spans and partial burial of the pipe. Sources of damage may stem from e.g. trawlers and anchor handling,[2] weather conditions such as hurricanes,[3] and erosions.

External inspection of pipelines has traditionally been handled by remotely operated vehicles (ROVs). These are tethered, unmanned vehicles controlled from a support vessel. Some of the problems of ROV inspection include the associated cost of having a large manned support vessel, a limited operating range in relation to the support vessel, limitations on which weather conditions the support vessel may operate in, and relatively slow speed due to on-line manual inspection of the pipeline.

Autonomous underwater vehicles (AUVs) may alleviate some of these issues, as AUVs are unmanned, untethered vehicles able to operate without a support vessel - they can operate unsupervised, or autonomously, for a long period of time. However, employing an AUV for pipeline inspection introduces some challenges. The AUV needs to navigate autonomously, inferring its own position, history, and goals. Furthermore, there is a need to track the pipeline position relative to the AUV in order to inspect it.

Further author information: (Send correspondence to G.M.B.)
G.M.B.: E-mail: goril.m.breivik@sintef.no, Telephone: +47 22 06 75 83
S.A.F.: E-mail: sigurd.fjerdingen@sintef.no, Telephone: +47 73 59 44 37
Ø.S.: E-mail: oystein.skotheim@sintef.no, Telephone: +47 73 59 70 47

Several research groups have focused on various aspects of autonomy and tracking for AUVs in the past. Research focus ranges from general AUV position estimation,[4] via detection and identification of general subsea structures,[5–7] to our target interest of pipeline or cable tracking.

For ROVs, Conte et al[6] tried a camera based solution in order to detect structural elements of a pipeline to ease the work of an operator. The pipe profile could also be detected. Balasuriya and Ura[8] fused data from a camera with an inertial navigation system (INS) and sonar data to track a pipeline. Experiments were carried out on the AUV 'Twin-burger 2'.[9] This is a similar application to the work of Antich and Ortiz,[10,11] which create a vision system and control architecture for pipe tracking.

Other sensors have also been tried for pipeline tracking. Inzartsev and Pavin[12,13] have used a multi-beam echo sounder to detect pipelines, as well have Evans et al[14] in conjunction with side-scan sonar in the EU funded project Autotracker. Recently Inzartsev and Pavin[15] used a video camera and what they call an electromagnetic searcher in order to solve the same problem.

The main contribution of this paper is the introduction of a method for pipeline localization based on a combination of two out of three available sensors, namely two color cameras and an echo sounder. The localization is performed using two different algorithms. The first algorithm is built on a common stereo vision approach and makes use of data from the two color cameras. The second algorithm exploit the echo sounder data at hand, and uses this in combination with either the left or the right camera for 3D localization relative to the AUV.

Hence, pipeline localization is done by utilizing data from either two color cameras, or one of the color cameras and the echo sounder. The latter approach assumes that the sea floor is close to horizontal in the area of interest. However, since the pipe often is lost in one of the camera images, and this approach enables localization of the pipe in such cases, the combination of the two algorithms is believed to constitute a more robust base for pipeline tracking over time.

The algorithms are evaluated in closed water recordings using an AUV developed for research purposes and pipelines with a diameter of 14 cm. The results from each of the three sensor combinations are compared to an auxiliary measured ground truth, and the accuracy of the approaches is presented. Finally, the algorithm robustnesses are compared in terms of number of true and false positive and negative pipeline localizations made during a recording simulating a pipe search procedure.

The two algorithms for pipeline detection in 3D are presented in Section 2. Section 3 describes the equipment, experimental procedure and statistical methods used for system evaluation. The accuracy and robustness results from the system evaluation are presented in Section 4. Section 5 discusses the most important results and the validity of them, before some conclusion are drawn and further work is presented in Section 6.

2. PIPELINE LOCALIZATION IN 3D

This section first describes the preliminary detection of the pipeline in the camera images, which is necessary before the localization algorithms are applied. Then the details for each of the two localization algorithms, the stereo vision approach and the echo sounder approach, are described.

2.1 Pipe detection in images

The pipe is segmented out in the camera images by thresholding using Otsu's method.[16] The thresholded image is then eroded using a disk of size 21 pixels in order to remove noise objects in the image, before edges are found using a Sobel filter.[17] The Hough transform[18] is used for detecting lines in the image, and line segments with a minimum length of 100 pixels, containing no gaps bigger than 40 pixels, are extracted. In the presence of two detected lines, the pipe is detected as the center line in the middle of these. This detection approach is based on the assumption that the pipe constitutes a straight line, and does not contain any sharp bends or intersections within the image. See Figure 1 for examples on the detection steps.

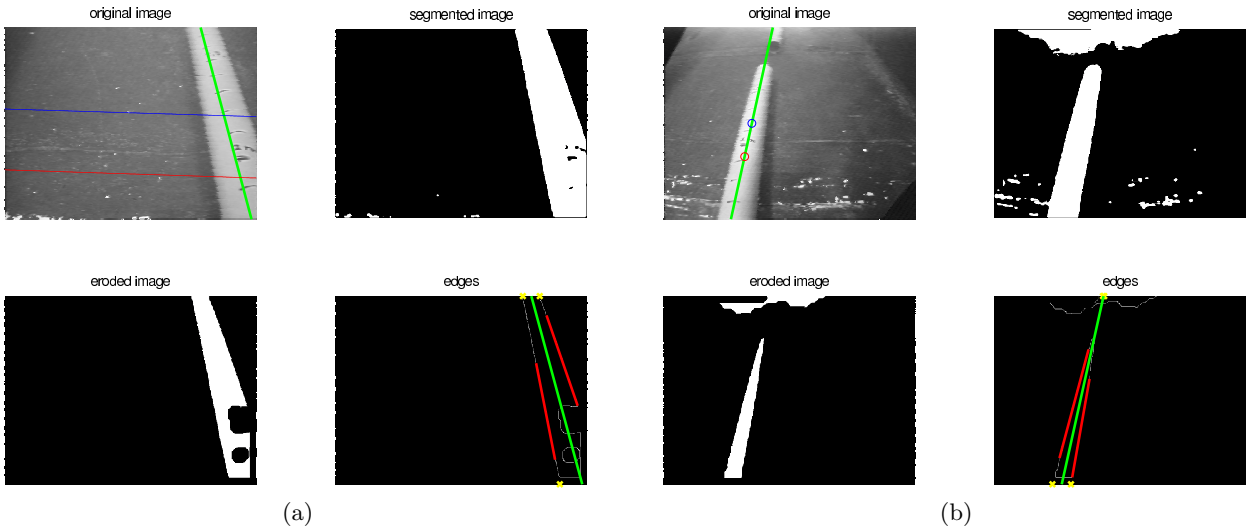

Figure 1: Images from the left (a) and the right (b) camera on the AUV (upper left images) and results after the segmentation (upper right), erosion (lower left) and line detection (lower right) steps in the pipe detection procedure. The green line indicates the detected pipeline. The blue and red circles in the upper right image in (b) correspond to the blue and red epipolar lines in the upper right image in (a). The intersection of the epipolar lines and the detected pipeline in (a) defines two points corresponding to the circles in (b).

2.2 Stereo vision approach

When the pipe is detected in both camera images, the stereo vision algorithm is used for pipeline localization in 3D. Stereo triangulation assumes the presence of corresponding point pairs in the two camera images. Finding such corresponding points on a pipeline with no easily distinguishable features is a challenge. Our solution to this is to use epipolar lines.[19] One point in the right image corresponds to a line, the epipolar line, in the left image. We take the point where this line intersects with the detected pipeline in the left image as the corresponding point to the original point in the right image.

The algorithm is based on taking the middle point and one point 100 pixels further down the pipe in the right image, and then finding the corresponding points in the left image, as can be seen in Figure 1. We now have two point pairs on the pipeline in the 2D images, and the pipe position in 3D can be found using stereo triangulation.[19] Two points on the pipeline in 3D clearly define a position relative to the AUV. For a mathematical representation of the pipe, we parameterize its position in 3D into a start point $\boldsymbol{x_0}$ and a direction vector $\boldsymbol{a}$: $\boldsymbol{x} = \boldsymbol{x_0} + \boldsymbol{a}\mathrm{t}$.

2.3 Echo sounder approach

The echo sounder approach for pipeline localization assumes the detection of a pipeline in only one of the camera images. The concept is that the detected center line in the camera image, when held together with the camera focal point, spans a plane in 3D with normal vector $\boldsymbol{n_1}$, as shown in Figure 2a. The sea floor spans a second plane with normal vector $\boldsymbol{n_2}$, and the pipe position in 3D is found as the intersection line of these two planes. Once again, the pipe is parameterized as a line in 3D, using a start point $\boldsymbol{x_0}$ and a direction vector $\boldsymbol{a}$.

The echo sounder provides continuous information of the depth from the AUV to the sea floor, and this is used to find the plane spanned by the sea floor. Hence, assumptions made for this approach to be valid, is that the sea floor is horizontal in the area of interest, i.e. in the local neighborhood from the AUV to the pipeline. The pipe is also assumed to lie close to horizontally. In the case when this assumption is not fulfilled, the estimated pipe position and angle will not be accurate, and the inaccuracy is expected to increase with deviation from the horizontal plane and distance to the detected pipeline. Moreover, an approximate diameter of the pipe should be known, as this represents an offset of the detected line above the sea floor.

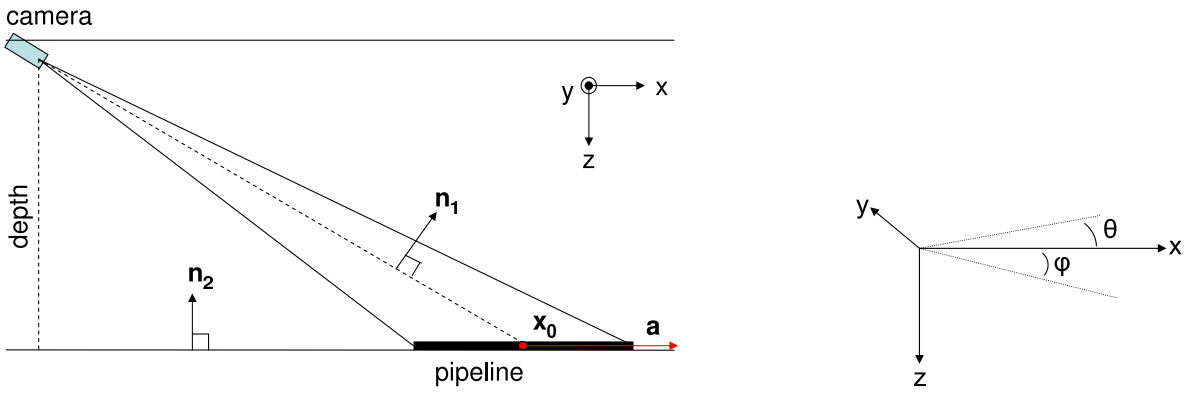

(a) (b)

Figure 2: (a) The concept of the echo sounder algorithm. The pipe is found as the intersection line of a plane $\boldsymbol{n_1}$ in 3D spanned by the pipeline and the camera, and a plane $\boldsymbol{n_2}$ spanned by the sea floor. (b) The coordinate system is defined with the x-axis in the horizontal speed direction of the AUV, the z-axis pointing vertically down, and with the y-axis pointing accordingly to the side defined by a right hand system. Origo is in the AUV left camera focal plane. The angle $\boldsymbol{\theta}$ is the horizontal angle relative to the x-axis, and the angle $\boldsymbol{\phi}$ is the vertical angle relative to the x-axis.

Figure 3: The AUV is a vehicle developed for research purposes, with a sensor package including two color cameras, echo sounder, sonar and an inertial measurement unit (IMU). A GPS mounted on an antenna on the AUV is available for test purposes and position verification while operating the AUV near the surface.

3. EXPERIMENTAL SETUP AND SYSTEM EVALUATION

The algorithms for pipeline localization in 3D were evaluated in a closed water experiment. This section outlines the equipment and procedures used during the tests, and methods used for statistical evaluation of the results.

3.1 System equipment

The AUV used during tests is a research vehicle developed for research purposes at SINTEF and the Norwegian University of Science and Technology. The vehicle dimension is 150 x 40 x 25 cm, and it has a weight of approximately 70 kg. The AUV sensor package includes two color cameras, echo sounder, sonar and an inertial measurement unit (IMU). A GPS mounted on an antenna on the AUV is available for test purposes and position verification while operating the AUV near the surface. See Figure 3 for a picture of the research AUV.

The underwater cameras are of type Kongsberg SIMRAD OE14-110 (Compact Colour CCD Camera, 73 degrees angle of view) and OE14-376 (Light Ring Colour Camera, 36 degrees angle of view), and are mounted outside of the vehicle due to mechanical reasons such as space limitations and maintenance of a waterproof hull. The wide angle camera is mounted on the right hand side, tilted with an approximate angle of 40 degrees towards the sea floor. The left camera is tilted with an approximate angle of 35. The reason for the difference in the tilt angles is inaccuracies in the mechanical adjustment of the cameras. However, since the left camera has a smaller angle of view than the right camera, the left camera image is still completely included in the right camera image in the vertical direction. The Tritech Micron Echo Sounder DST, mounted underneath the vehicle at a 5 cm distance below the cameras, has an operating range up to 50 meters and a 1 mm resolution accuracy.

The sensor system was first tested in an open water environment, for detecting pipelines of various colors and diameters at 1-2 meter depth. The pipe detection algorithm was developed based on data from these recordings. For evaluation of the proposed localization algorithms, however, recordings were performed in a pool. Such a closed environment facilitated ground truth measurement for accuracy evaluation, which was our primary focus in this phase of the project. The pool recordings were performed at an approximate depth of 1 meter, recording orange pipes with a diameter of 14 cm and length 2 m.

3.2 Experimental procedure

For accuracy measurement of the proposed algorithms, one series of well controlled recordings were performed. In the series, the AUV was placed in four different positions relative to the pipe. The exact AUV position relative to the pool and pipeline was measured for each position. Other distances, such as depth from cameras to the pool floor and camera angles were measured accordingly. The positioning and heading of the AUV at all times were ensured using two metal rods at a fixed distance from the pool edge. Sensor data from left and right camera, echo sounder and IMU were recorded for a few seconds in each position, providing a total of four sets of pipe position measurements and their corresponding ground truths.

For algorithm robustness evaluation, one measurement series was taken while the AUV was running in a random path in the pipeline neighborhood, simulating a pipe search procedure. A total of 150 images were taken with each of the cameras, and the pipeline was present in at least one of the camera images most of the time. The pipe localization robustness for each of the algorithms was compared based on this recording, by counting the the number of true and false positive and negative pipe localizations.

3.3 Statistical analysis

The accuracy of the estimated pipe localizations is evaluated at a 1 meter distance from the AUV. The coordinate system is defined with the x-axis in the horizontal speed direction of the AUV, the z-axis pointing vertically down, and with the y-axis pointing accordingly to the side defined by a right hand system. Origo lies in the AUV left hand camera focal plane. For the plane x = 1 meter, the estimated y- and z-positions of the pipe are evaluated for each of the algorithms, and compared to the ground truth position of the pipe. In the same plane, the horizontal angle $\boldsymbol{\theta}$ and vertical angle $\boldsymbol{\phi}$ of the pipe are evaluated. See Figure 2b.

Scatter plots of the position $(\boldsymbol{y}, \boldsymbol{z})$ and angle $(\boldsymbol{\theta}, \boldsymbol{\phi})$ show the estimated pipe position for the three sensor combinations: stereo vision, left camera combined with echo sounder and right camera combined with echo sounder. The plots give an idea of mean and variance in the results for each of the algorithms, and facilitates comparison to ground truth measurement for each of the four positions in the accuracy measurement. Studying the deviation from the ground truth makes it possible to report a mean and spread for each algorithm based on all the measurements.

Robustness of each of the algorithms is evaluated as a measure of false and true negative and positive localizations in the pipe search recording. False localizations means that the pipe is not localized, or the localization of the pipe is wrong. This is determined based on visual observations of each image, and images where pipe detection is outside of the pipeline are characterized as negative localizations. On the other hand, true localizations are correct localizations of the pipe. Negative localization means that the pipe is detected as not present, while positive localization means that the pipe is present.

As the pipe detection procedure is not optimized, the algorithms are expected to perform poorly when it comes to absolute detection rate. However, an interesting measure is the relative detection rate when comparing

Table 1: Mean and spread in estimated pipe position and angle, when compared to ground truth, for each of the three sensor combinations. Mean $\boldsymbol{\mu}$ is divided into one horizontal and one vertical component. Average mean is computed as length of the mean vector. Spread $\boldsymbol{\sigma}$ is found from the covariance matrices for each of the data sets.

Mean and spread	**Left cam+echo sounder**	**Right cam+echo sounder**	**Stereo camera**
Avg mean position (μ_{yz})	7.8 cm	16.7 cm	7.7 cm
Mean position (μ_y, μ_z)	(7.3, -2.8) cm	(16.3, 3.6) cm	(7.1, -2.9) cm
Spread position (σ_1, σ_2)	(3.4, 14.9) cm	(3.3, 26.3) cm	(12.6, 20.5) cm
Avg mean angle ($\mu_{\theta\phi}$)	1.1 deg	2.9 deg	3.3 deg
Mean angle (μ_θ, μ_ϕ)	(1.1, 0) deg	(1.9, 2.2) deg	(-0.83, -3.2) deg
Spread angle (σ_1, σ_2)	(0, 4.8) deg	(0, 7.3) deg	(3.7, 9.1) deg

the stereo vision algorithm to the approaches based on echo sounder data. In particular, we expect a higher true positive detection rate when applying the novel approach, at the same time as we assume the false negative detection rate will be lower, since the echo sounder algorithm is not dependent on pipe detection in both camera images at the same time.

4. RESULTS

Figure 4 shows the estimated pipe position in 3D for the third position in the accuracy recording. Positive direction for the z-axis is down, but the numbers on the axis indicate the opposite due to the plotting procedures in Matlab. This is accounted for by labeling the axis -z.

Pipe positions estimated using the stereo vision algorithm are shown in red, results in blue are based on the left camera and echo sounder, and results in green are based on the right camera combined with echo sounder data. Ground truth is indicated with a black line, and origo is indicated by a red circle. The pipe position is also shown as seen from above (Figure 4b), from the side (Figure 4c) and from behind (Figure 4d).

4.1 Accuracy

Scatter plots of the estimated pipe position $(\boldsymbol{y}, \boldsymbol{z})$ and angle $(\boldsymbol{\theta}, \boldsymbol{\phi})$ in the plane x = 1 meter are shown in Figure 5. Figure 5a-5d show results from the measurements taken in AUV position 1-4, respectively. In these plots, the ground truth is indicated by a black circle, and origo is indicated by a red circle. Stereo results are shown in red, left camera results in blue and right camera results in green.

Figure 6 is similar to the plots in Figure 5. However, here results from all the four positions are assembled into one plot by accounting for the ground truth position for each one of them. Hence, the ground truth is now in origo for the $(\boldsymbol{y}, \boldsymbol{z})$- and $(\boldsymbol{\theta}, \boldsymbol{\phi})$-plots.

Deviations from the ground truth for each of the algorithms are found as mean and spread of the measurements in Figure 6. For each of the sensor combinations, the mean value along each of the axis is computed. Hence, deviations from the ground truth is divided into one horizontal and one vertical component in both position and angle. An average deviation mean is found as the length of the mean vectors.

Spread in the measurements is found as the square root of the eigenvalues of the data covariance matrices. This results in a two dimensional vector, indicating the spread along the two main axis of the data sets, regardless of data set orientation. Table 1 summarizes the mean and spread in estimated position and angle for each of the three sensor combinations.

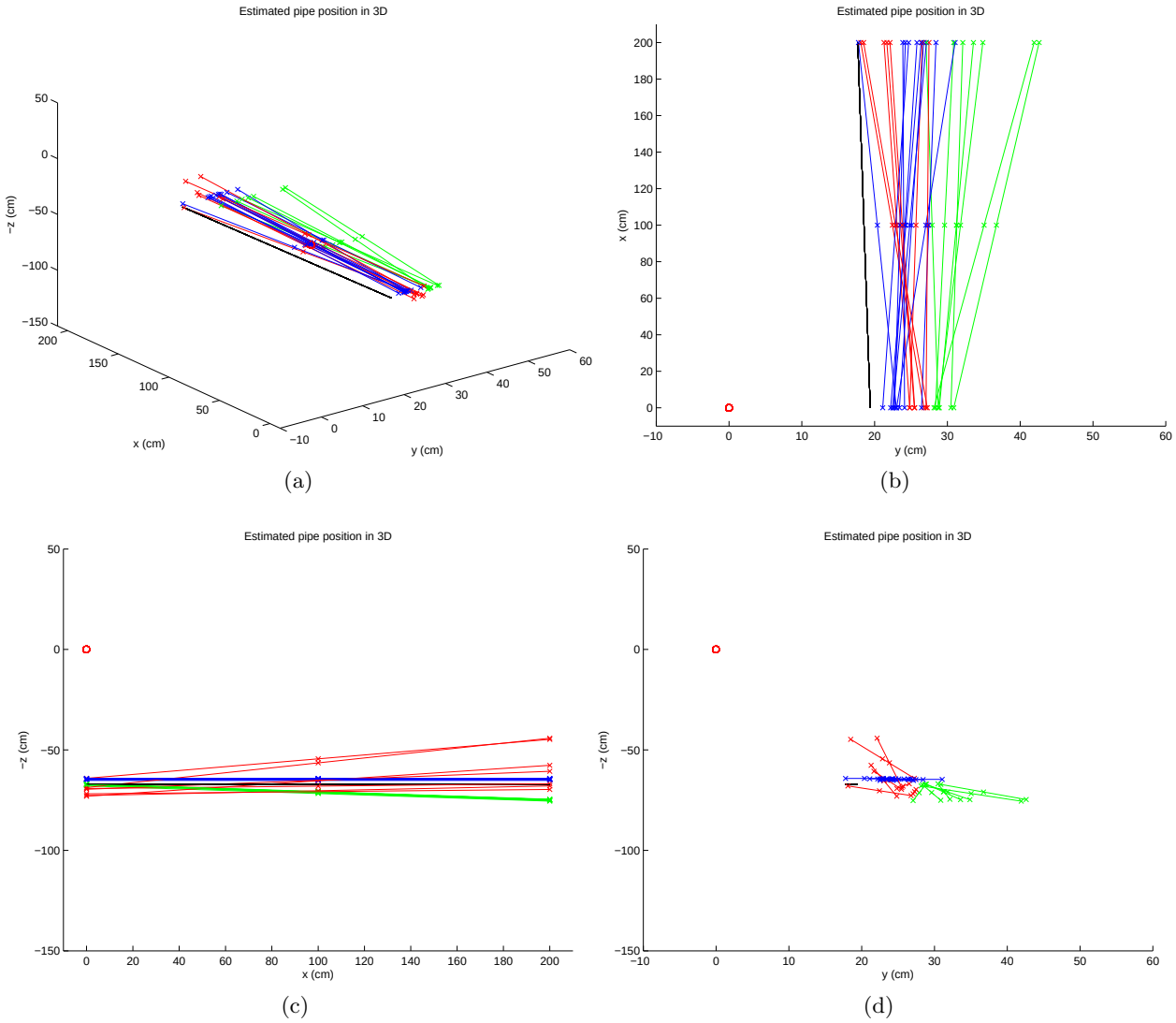

Figure 4: Estimated pipeline positions in 3D relative to the AUV when the AUV is placed in position no. 3, seen from above (b), the side (c) and behind (d). Pipeline positions are estimated using the stereo vision approach (red) and the echo sounder in combination with left (blue) and right (green) camera. Ground truth is indicated by a black line. Origo is in the left camera focal point, and is indicated by a red circle. Positive direction for the z-axis is down. Crosses on the lines indicate x = 0 m, 1 m and 2 m.

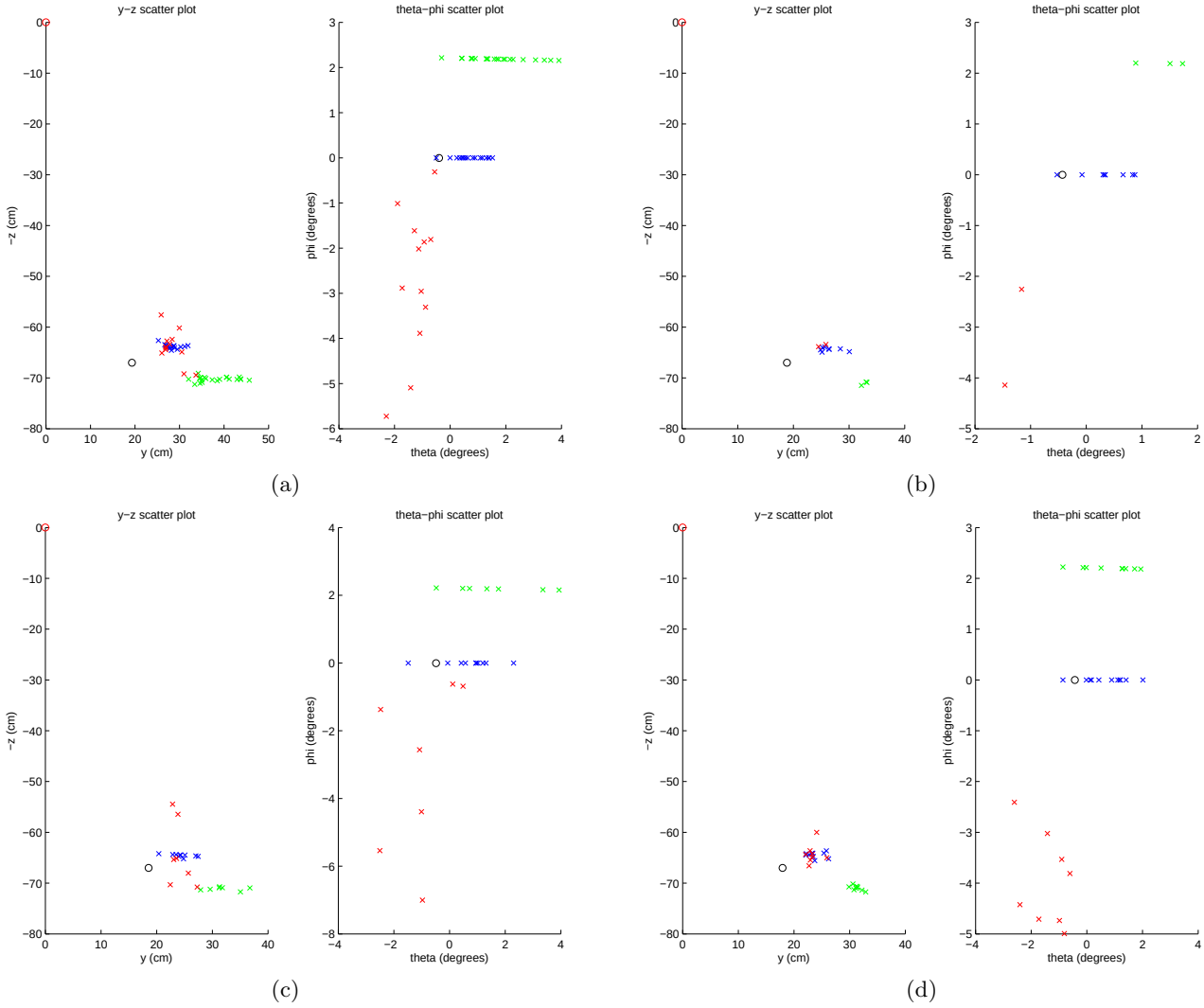

Figure 5: Estimated pipe position (y, z) to the left and bearing (θ, ϕ) to the right at x=1 meter distance from origo when the AUV is placed at four different positions along the pipeline (a = pos. 1, b = pos. 2, c = pos. 3, d = pos. 4). Estimations are based on the stereo vision approach (red), the echo sounder in combination with left (blue) and right (green) camera. Ground truth is indicated by a black circle, and origo is indicated by a red circle.

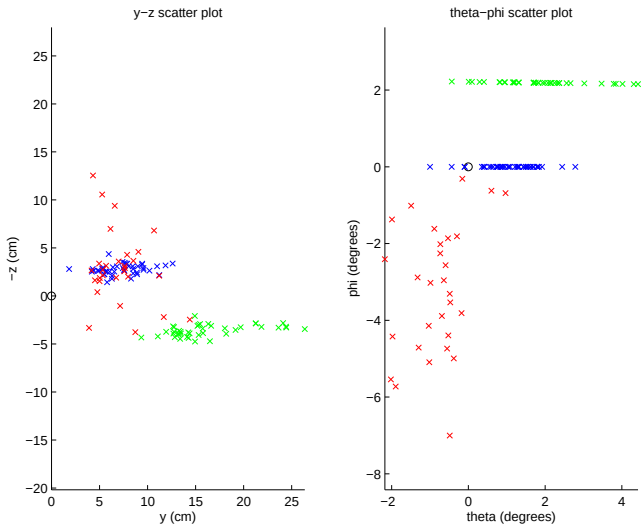

Figure 6: Deviations from the ground truth in estimated pipe position $(\boldsymbol{y}, \boldsymbol{z})$ to the left, and pipe angle $(\boldsymbol{\theta}, \boldsymbol{\phi})$ to the right, in a plane at x = 1 meter. Stereo vision results in red, echo sounder combined with left camera results in blue and echo sounder combined with right camera results in green. Ground truth indicated by a black circle in origo.

Table 2: The percentage of false and true negative and positive pipe localizations for the three sensor combinations. When applying both the left and right camera in combinations with echo sounder data, the true positive detection rate is increased by a factor four, compared to stereo vision algorithm.

Statistics	**Left cam/echo sounder**	**Right cam/echo sounder**	**Stereo camera**
True positives	26 %	40 %	13 %
False positives	11 %	7 %	7 %
True negatives	25 %	5 %	30 %
False negatives	37 %	47 %	50 %
True pos. (left+right)	53 %	53 %	13 %
True pos. (theoretically)	71 %	95 %	69 %
True pos. (theo.left+right)	97 %	97 %	69 %

4.2 Robustness

The number of true and false positive and negative localizations of the pipeline is evaluated by visual inspection of each image and the corresponding algorithm output for the robustness recording. Table 2 summarizes the results. The absolute percentages reported in this table show that there is a theoretical chance of up to 71 % true positive detections for the left camera with echo sounder, 95 % for the right camera with echo sounder and 69 % for the stereo camera. Moreover, when pipe localizations is based on *either* the left or the right camera together with echo sounder data, the number of true positive localizations is increased to 53 %, which is a factor four higher than the stereo vision results of 13 %.

In Figure 7 the localization results are plotted into a receiver operating characteristic (ROC) curve. Figure 7a shows the true positive rate versus false positive rate and Figure 7b shows the true negative versus false negative rate for each of the three sensor combinations. Results in the left curves should ideally lie as close to the vertical axis as possible, and at the same time as high as possible on this axis, as this would mean a high detection rate of true positives, while keeping the false positives as low as possible. In the right curve, the results should lie close to the vertical axis, but as low as possible, since the pipeline is expected to be present in most of the images.

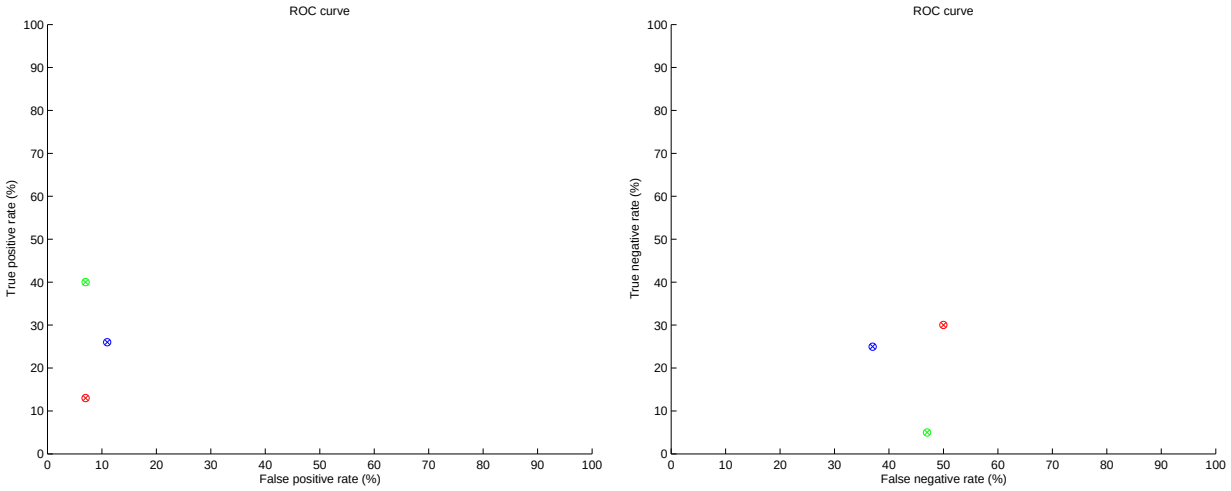

(a) (b)

Figure 7: A receiver operating characteristic (ROC) curve showing (a) the true positive versus false positive localization rate and (b) the true negative versus false negative localization rate for the left camera in combination with echo sounder (blue), right camera in combination with echo sounder (green) and the stereo camera algorithm (red). Results should ideally lie close to and high up on the vertical axis in (a), and close to and low on the vertical axis in (b).

5. DISCUSSION

5.1 Summary of the results

The accuracy measurements in Figure 5 show that the three sensor combinations give consistent results for each of the four AUV positions in the recordings. This is confirmed in Figure 6, where the results are unified after compensating for the ground truth position of the pipe.

Results from the stereo vision algorithm seem to coincide well with results using the left camera in combination with the echo sounder. The right camera and echo sounder results seem to deviate slightly from the other results, in the $(\boldsymbol{y}, \boldsymbol{z})$-plot in Figure 6. A reason for this might be the manual measurement of camera rotation angle and compensations made for this in the algorithms. A more exact modeling of the camera positions relative to each other and to the AUV, based on extrinsic calibration results, would probably give more similar results from the left and right camera systems.

The $(\boldsymbol{\theta}, \boldsymbol{\phi})$-plot in Figure 6 shows a greater spread in the results for the stereo algorithm than for angles estimated based on the echo sounder approach. The zero variance in the $\boldsymbol{\phi}$-direction of the results is however a natural consequence of the assumptions the echo sounder algorithm is based on, namely that the pipeline is assumed to lie horizontally on the sea floor. Hence a bigger variation for the stereo camera approach, which does not have this restriction, is expected, although a variation up to 9 degrees is more than what is desirable for such systems. The difference in estimated pipe angle for the left and right camera systems is a result of the slightly different rotation angles of the cameras, and the choice of coordinate system definition in the left camera focal point.

The robustness evaluation of the algorithms, visualized in Figure 7, show that the echo sounder algorithms for left and right cameras perform better than the stereo vision algorithm for the left ROC curve. The maximum theoretical percentage of true positive detections is higher when the algorithms depend on pipe detection in only one and not two cameras at the same time. Hence, such an improved performance in true positive detection rate of the one camera plus echo sounder algorithm is as expected. In particular, combining the two echo sounder algorithms results in a true positive rate of 53 %, which is four times better than the 13 % performance of the stereo algorithm.

The true versus false negative results to the right in Figure 7 show a rather poor performance for all of the algorithms, as the false negative rate is relatively high for all cases. This is assumed to be as a result of an immature procedure used for pipe detection before the localization algorithms are applied. The pipe detection procedure has a great potential for improvement, however at this stage of the project focus has been on the localization procedures. Hence, the interesting aspect is the relative performance of the algorithms. The stereo vision approach has the highest false negative rate, which is natural since this algorithm is more sensitive to a lack of pipe detection in one of the camera images. The true negative rate of localizations is low for the left camera, meaning that the pipe is rarely missed from this camera in the recording.

5.2 Validity of the results

There were difficulties in performing auxiliary measurements in order to clearly define the pipeline ground truth position and AUV position relative to the pipeline at all times. The measurements were done using a tape measure, which gave inaccurate results in many cases due to e.g. challenges in holding the measure in a completely horizontal and vertical position. Moreover, holding the pipeline and especially the AUV still in the water at all times during the measurements and data recordings turned out to be very hard. Due to these difficulties during the experiment, the ground truth measurements are not fully trustworthy.

Nevertheless, the stereo vision and left camera results seem to coincide well in the position plot in Figure 6, and the slightly deviating results from the right camera algorithm might be explained by poor measurements of the camera orientations relative to each other. This gives confidence in the achieved results for both algorithms. The variations between 3 and 26 cm in pipe position is a rather poor result. However, the accuracy is in an order comparable to the pipe diameter of 14 cm, and as a first result in our pipe localization work in progress, this is a localization accuracy usable for our present needs.

The spread in estimated pipe angle in Figure 6 gives rise to some concerns. Especially the results from the stereo vision approach are not as good as expected, with an average deviation angle of 3.3 degrees and spread up to 9 degrees. However, these variations are believed to come from the challenges in holding the AUV still in the water during the recordings. An easy solution to this would be to account for movements using measurements from the inertial measurement unit (IMU) mounted on the vehicle. Correction for roll, pitch and yaw is not implemented in the algorithms yet, but is believed to improve the results.

The immature and not very optimized pipe detection algorithm used on the camera images affects the robustness performance of the algorithms. Moreover, it will affect the algorithm that is more sensitive to simultaneous detection of pipes in both image, i.e. the stereo vision algorithm, more than the echo sounder approach. Nevertheless, the theoretical limit of true positive localizations is higher for the echo sounder approach than for the stereo vision approach, due to the fact that the pipeline is visible in one of the camera images more often than it is visible in both images at the same time. Hence, the echo sounder algorithm is believed to provide a higher true positive detection rate than the stereo vision algorithm, regardless of the performance of the pipe detection procedure.

6. CONCLUSION

In this paper we have presented two algorithms for pipeline localization in 3D based on three sensor combinations: stereo camera, left camera with echo sounder and right camera with echo sounder. The results imply that the combination of one camera and echo sounder data can be used for pipeline localization in 3D, as the accuracy of the echo sounder algorithm is comparable to that resulting from the stereo vision algorithm.

The echo sounder approach is built on the assumption that the sea floor and pipe angle are close to horizontal in the area of interest. Moreover, both algorithms have shown to be vulnerable to movements in the vehicle during recordings. This affects the localization accuracy and introduces some limitations in the usability of the algorithms.

The echo sounder algorithm provides a true positive localization rate four times better than the stereo vision algorithm, and also better true and false negative rates. As a result, a combination of the echo sounder approach with the stereo vision approach is believed to give a more robust pipe localization system for the AUV, facilitating tracking of pipelines over time.

6.1 Further work

Implementation of a couple of steps is believed to improve the performance of both the stereo vision and the echo sounder algorithms. First, this includes a better and more accurate modeling and measurement of the position and rotation of the cameras relative to each other, which can be done based on extrinsic camera calibration. Second, correcting for movements of the vehicle during measurements using data from the inertial measurement unit is believed to produce more stable pipeline localization measurements over time.

ACKNOWLEDGMENTS

The authors thank Jens T. Thielemann for helpful discussions in the initial development of algorithm concepts.

REFERENCES

[1] [*Utbygging og drift av Ormen Lange og anlegg og drift av Langeled m.v.*], The Norwegian oil and energy authority, St.prp. 41 (2003-2004) (2003).

[2] [*Small gas leak from Kvitebjrn pipeline*], www.statoilhydro.com [cited 30.10.2009], StatoilHydro News Report (2008).

[3] [*Pipeline Damage Assessment from Hurricanes Katrina and Rita in the Gulf of Mexico*], DNV technical report no. 44814183 (2008).

[4] Kalyan, B. and Balasuriya, A., "Multiple sensors based navigation scheme for auv position estimation," in [*2004 International symposium on underwater technology*], 201–207 (April 2004).

[5] Trucco, E. and Plakas, K., "Video tracking: A concise survey," *IEEE Journal of oceanic engineering* **31**, 520–529 (April 2006).

[6] Conte, G., Zanoli, S., Perdon, A. M., Tascini, G., and Zingaretti, P., "automatic analysis of visual data in submarine pipeline inspection," in [*OCEANS'96 MTS/IEEE conference proceedings*], **3**, 1213–1219 (1996).

[7] Messina, L. C. P., Simoes, A. P., Botto, A., and Petraglia, A., "Three dimensional imaging system for subsea inspection," in [*Proceedings of the 25th international conference on offshore mechanics and arctic engineering*], **4**, 343–352, American Society of Mechanical Engineers (2006).

[8] Balasuriya, A. and Ura, T., "autonomous underwater vehicle navigation scheme for cable following," in [*Proceedings of the 2001 IEEE Intelligent transportation systems*], 519–524, IEEE (2001).

[9] Balasuriya, A. and Ura, T., "Autonomous underwater vehicles for submarine cable inspection: experimental results," in [*2001 IEEE Conference on systems, man, and cybernetics*], **1**, 377–382, IEEE (October 2001).

[10] Ortiz, A., Sim, M., and Oliver, G., "A vision system for an underwater cable tracker," *Machine vision and applications* **13**, 129–140 (July 2002).

[11] Antich, J. and Ortiz, A., "Development of the control architecture of an underwater cable tracker," *International journal of intelligent systems* **20**, 477–498 (March 2005).

[12] Inzartsev, A. V. and Pavin, A. M., "Auv behavior algorithm while inspecting of partly visible pipeline," in [*OCEANS 2006*], 1–5, IEEE (September 2006).

[13] Pavin, A. M., "The pipeline identification method basing on auv's echo-sounder data," in [*OCEANS 2006*], 1–6, IEEE (2006).

[14] Evans, J., Petillot, V., Redmond, P., Reed, S., and Lane, D., "Autotracker: Real-time architecture for pipeline and cable tracking on auvs," in [*Guidance and control of underwater vehicles 2003*], *IFAC Workshop series*, 241–246, Elsevier science BV (2003).

[15] Inzartsev, A. V. and Pavin, A. M., "Auv cable tracking system based on electromagnetic and video data," in [*OCEANS 2008*], 1–6, IEEE (April 2008).

[16] Otsu, N., "A threshold selection method from gray-level histograms," *IEEE Trans. Sys., Man., Cyber.* **9**, 62–66 (1979).

[17] Duda, R. and Hart, P., [*Pattern Classification and Scene Analysis*], John Wiley and Sons (1973).

[18] Duda, R. and Hart, P., "Use of the hough transformation to detect lines and curves in pictures," *Comm. ACM* (1972).

[19] Sonka, M., Hlavac, V., and Boyle, R., [*Image Processing, Analysis and Machine Vision*], PWS Publishing (1998).